nature geoscience

LETTERS

PUBLISHED ONLINE: 7 SEPTEMBER 2015 | DOI: 10.1038/NGEO2514

Rainfall consistently enhanced around the Gezira Scheme in East Africa due to irrigation

Ross E. Alter[1*†], Eun-Soon Im[2*†] and Elfatih A. B. Eltahir[1]

Land-use and land-cover changes have significantly modified regional climate patterns around the world[1,2]. In particular, the rapid development of large-scale cropland irrigation over the past century has been investigated in relation to possible modification of regional rainfall[3–14]. In regional climate simulations of the West African Sahel, hypothetical large-scale irrigation schemes inhibit rainfall over irrigated areas but enhance rainfall remotely[13,14]. However, the simulated influence of large-scale irrigation schemes on precipitation patterns cannot be substantiated without direct comparison to observations[15]. Here we present two complementary analyses: numerical simulations using a regional climate model over an actual, large-scale irrigation scheme in the East African Sahel—the Gezira Scheme—and observational analyses over the same area. The simulations suggest that irrigation inhibits rainfall over the Gezira Scheme and enhances rainfall to the east. Observational analyses of rainfall, temperature and streamflow in the same region support the simulated results. The findings are consistent with a mechanistic framework in which irrigation decreases surface air temperature, causing atmospheric subsidence over the irrigated area and clockwise wind anomalies (in background southwesterly winds) that increase upward vertical motion to the east. We conclude that irrigation development can consistently modify rainfall patterns in and around irrigated areas, warranting further examination of potential agricultural, hydrologic and economic implications.

Increases in soil moisture and plant growth due to cropland irrigation cause well-defined changes to local energy and moisture budgets[1,2,16,17]. Both numerical modelling and observational analyses have indicated that irrigation can decrease sensible heat flux and air temperature[4,5,7–9,12,14,18,19], increase latent heat flux and evapotranspiration[5,7–12,14,19,20], enhance low-level atmospheric moisture[5,8–10,12,21], and alter regional wind patterns[10,12–14,18,19]. In the United States[3,4,6,8–10,12], India[5], and other world regions with large irrigated areas[7,11,13,14], irrigation development has also been investigated in relation to increases[3–14] and decreases[5,7–9,12–14] in rainfall, both locally and remotely. Accurately diagnosing the influence of this 'irrigation effect'[4] on rainfall is essential for a complete understanding of anthropogenic impacts on regional climate systems.

In this study, we examine irrigation effects on rainfall within the African Sahel—a climatic transition region between the Sahara desert to the north and the more wooded savannah to the south. Irrigation in the African Sahel is investigated for several reasons: there exists considerable potential for future large-scale irrigation projects given the right combination of socioeconomic interests[22]; the economies of many countries in the African Sahel are strongly dependent on agriculture[23]; the effects of irrigation on energy and moisture budgets would probably be easily distinguishable from the typically hot and dry background climate; and previous studies have already identified potential rainfall enhancement in the West African Sahel due to hypothetical, large-scale irrigation development[13,14].

However, as no comparable large-scale irrigation projects exist at present in West Africa for observational validation, we focus on a large-scale irrigated area within the East African Sahel—the Gezira Scheme in central Sudan—which is situated just south of the confluence of the Blue Nile and White Nile rivers (Supplementary Fig. 1). Irrigation development in the Gezira Scheme began in 1925 and continued gradually until a major expansion between 1958 and 1962 (the Manaqil Extension—MEX) nearly doubled the irrigated area. Irrigated cropland in Gezira continued to increase gradually to a maximum of approximately 890,000 ha in 2008 (data obtained from the Ministry of Water Resources and Electricity of Sudan; Fig. 1c), making it the second-largest contiguous irrigation scheme in Africa. Its breadth, spatial continuity, rapid development (MEX) and location in an arid/semi-arid climate increase the likelihood that the Gezira Scheme has caused distinct and perceptible changes in regional temperature and rainfall.

Our objectives are to quantify the contribution of irrigation from the Gezira Scheme to local and regional rainfall changes and to validate these changes using observation-based data from the area. First, we used a regional climate model[24] (see Methods) to simulate control (non-irrigated) and irrigated scenarios and their difference over Sudan and neighbouring countries (Fig. 1a). Three ensemble runs were conducted with 20-km horizontal grid increments between 1979 and 2008 (90 total model years). An irrigation land-use category was applied to all of the Gezira Scheme and also to the New Halfa irrigation scheme to the northeast of Gezira (Fig. 1a). Within the model, irrigation was prescribed from July until September of each year, corresponding with irrigated periods of several major crops[25] and overlapping with the African monsoon, which delivers most of the annual rainfall to the Gezira area. Because irrigation and peak rainfall concur in July and August, it is during these months that we expect the largest impact on rainfall amounts.

Analyses of mean temperature and control rainfall preliminarily suggest that the Gezira Scheme influences regional energy and moisture budgets. Figure 1b depicts mean July–September daytime land surface temperature in the Gezira region derived from MODIS (Aqua satellite)[26] for 2003 to 2014. The Gezira and New Halfa schemes show clear temperature signals: land surface temperatures within the irrigation schemes are generally 3–5 K lower than in

[1]Ralph M. Parsons Laboratory, Massachusetts Institute of Technology, Cambridge, Massachusetts 02139, USA. [2]Center for Environmental Sensing and Modeling, Singapore—Massachusetts Institute of Technology Alliance for Research and Technology, Singapore 138602, Singapore. †These authors contributed equally to this work. *e-mail: ralter1@mit.edu; eunsoon@smart.mit.edu

© 2015 Macmillan Publishers Limited. All rights reserved

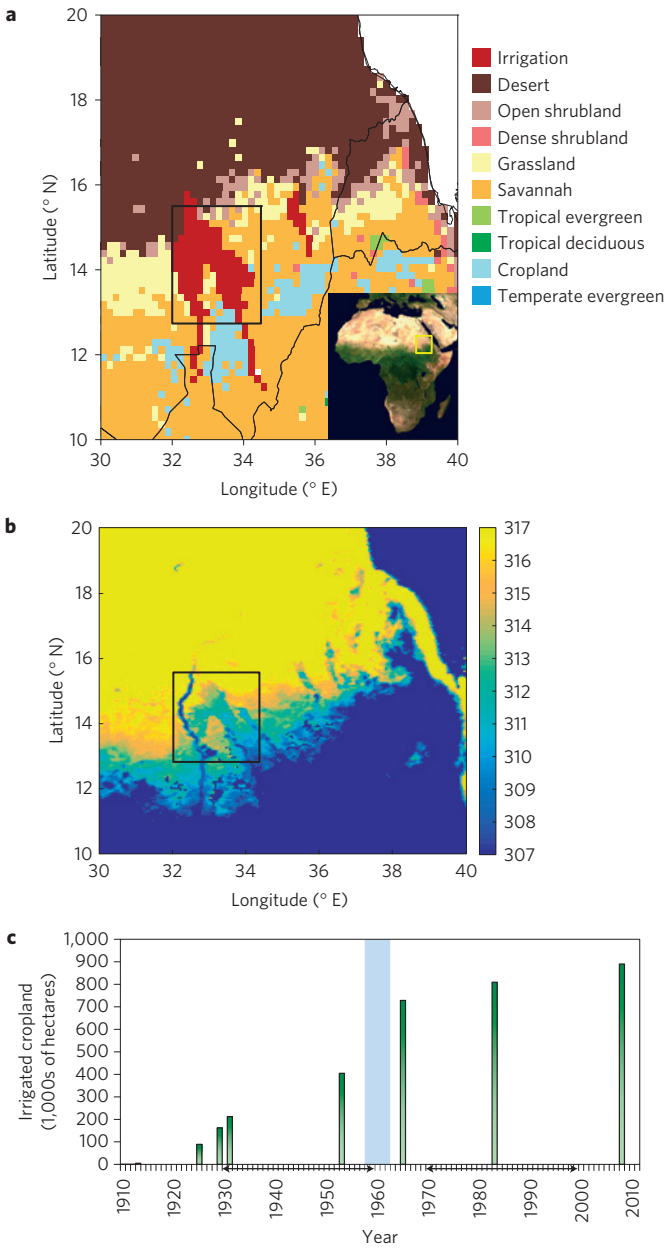

Figure 1 | Background information regarding irrigation in the Gezira Scheme. a, Dominant land-use categories within the model domain. A black rectangle is drawn around the Gezira Scheme. Inset, Satellite image of Africa with model domain indicated by the yellow box (© NASA). **b**, Mean daytime land surface temperature (K) for July–September from MODIS (Aqua satellite) over the period 2003–2014. **c**, Temporal evolution of irrigated cropland in the Gezira Scheme (thousands of hectares). The blue vertical bar represents the Manaqil Extension (MEX), a period of intense irrigation development between 1958 and 1962. Horizontal arrows below the *x*-axis indicate pre-MEX (1930–1959) and post-MEX (1970–1999) time periods. Data obtained from the Ministry of Water Resources and Electricity of Sudan.

the surrounding areas. Furthermore, comparing the mean rainfall of the control simulation with that of a gridded observational data set[27] reveals that the control experiment under-predicts a 'bulge' of rainfall to the southeast of Gezira in July and August (Supplementary Fig. 2) that does not seem to be greatly influenced by topography (Supplementary Fig. 1). As this isolated 'bulge' is the only major area of under-predicted rainfall in the model domain, it seems more probable that a localized forcing is the cause of this anomaly.

Indeed, spatial maps of simulated rainfall differences reveal that irrigation creates a 'bulge' of enhanced rainfall in nearly the same location as the under-predicted 'bulge'. When averaged over the three 30-year ensemble runs, rainfall during July and August is enhanced by 5–20% (0.1–1.0 mm d^{-1}) in a broad area extending east of the Gezira and New Halfa schemes into Eritrea and northern Ethiopia (Fig. 2a,b and Supplementary Fig. 3). For individual model years, irrigation enhances ensemble mean rainfall by up to 60% (3 mm d^{-1}) to the east of the Gezira Scheme (not shown). The consistency of these rainfall increases is also striking: in two distinct clusters of grid cells to the east of the Gezira Scheme, irrigation enhances rainfall during at least 70% of the 90 ensemble years (significant at the 1% level using the chi-square test). Furthermore, the robust decreases in rainfall over the irrigated areas match the pattern exhibited in previous studies of West Africa at similar latitude bands[13,14].

To verify that these theoretical changes in rainfall represent reality, we then compared the results of the simulations against observational data. Observational analysis was first performed using a gridded data set from the University of Delaware (UDel; ref. 27), which assimilates historical precipitation observations into 0.5° × 0.5° grid cells. Maps depicting the percentage and absolute changes in UDel July and August rainfall from pre-irrigation expansion (pre-MEX, 1930–1959) to post-irrigation expansion (post-MEX, 1970–1999) concur with the results of the modelling simulations: Rainfall exhibits anomalously strong decreases over the Gezira Scheme and distinct relative increases directly east of and further to the east-northeast of Gezira (Fig. 2c,d and Supplementary Fig. 3).

We focus on relative increases in rainfall because a multi-decadal drought in the Sahel post-MEX caused strong, region-wide decreases in rainfall that probably masked the absolute increases due to irrigation alone. However, despite this background influence, these relative increases in rainfall east of Gezira are still persistent: values of a consistency index for the observed rainfall changes in these areas (see Methods) are greater than 80% of all grid cell values (Fig. 2 and Supplementary Fig. 3). Therefore, the rainfall increases seem to be consistent in both the observations and simulations. The two clusters of observed and simulated rainfall increases are also nearly identical in location, with a margin of error of ±2 arc degrees. Thus, the spatial maps from UDel observations seem to support the major irrigation-induced changes in rainfall simulated by the model.

Observational verification of the simulated changes is also performed with monthly precipitation data from the Global Historical Climatology Network (GHCN; ref. 28) at six long-term stations in and around Gezira. The spatial differences in normalized July GHCN rainfall from pre-MEX to post-MEX match those of the modelling experiments—that is, relative decreases over the irrigated stations and relative increases to the east of the Gezira Scheme (Fig. 3c). Furthermore, time series of July GHCN rainfall at Gedaref (a non-irrigated station east of Gezira) and Wad Medani (an irrigated station within Gezira) and their difference indicate significantly greater rainfall in Gedaref relative to Wad Medani shortly after the MEX (vertical blue bar; Fig. 3a,b). Similar features are present in a GHCN analysis for August (Supplementary Fig. 4). These spatial and temporal signatures further suggest that irrigation in the Gezira Scheme has reduced rainfall over and enhanced rainfall adjacent to the irrigated areas.

The mechanistic linkages between Gezira irrigation and rainfall enhancement are further examined through analyses of changes in surface air temperature. Long-term surface air temperature data back to 1948 are derived from the NCEP–NCAR reanalysis[29]. Temporal changes are compared between three grid cells: one covering the Gezira Scheme (irrigated), one affected

© 2015 Macmillan Publishers Limited. All rights reserved

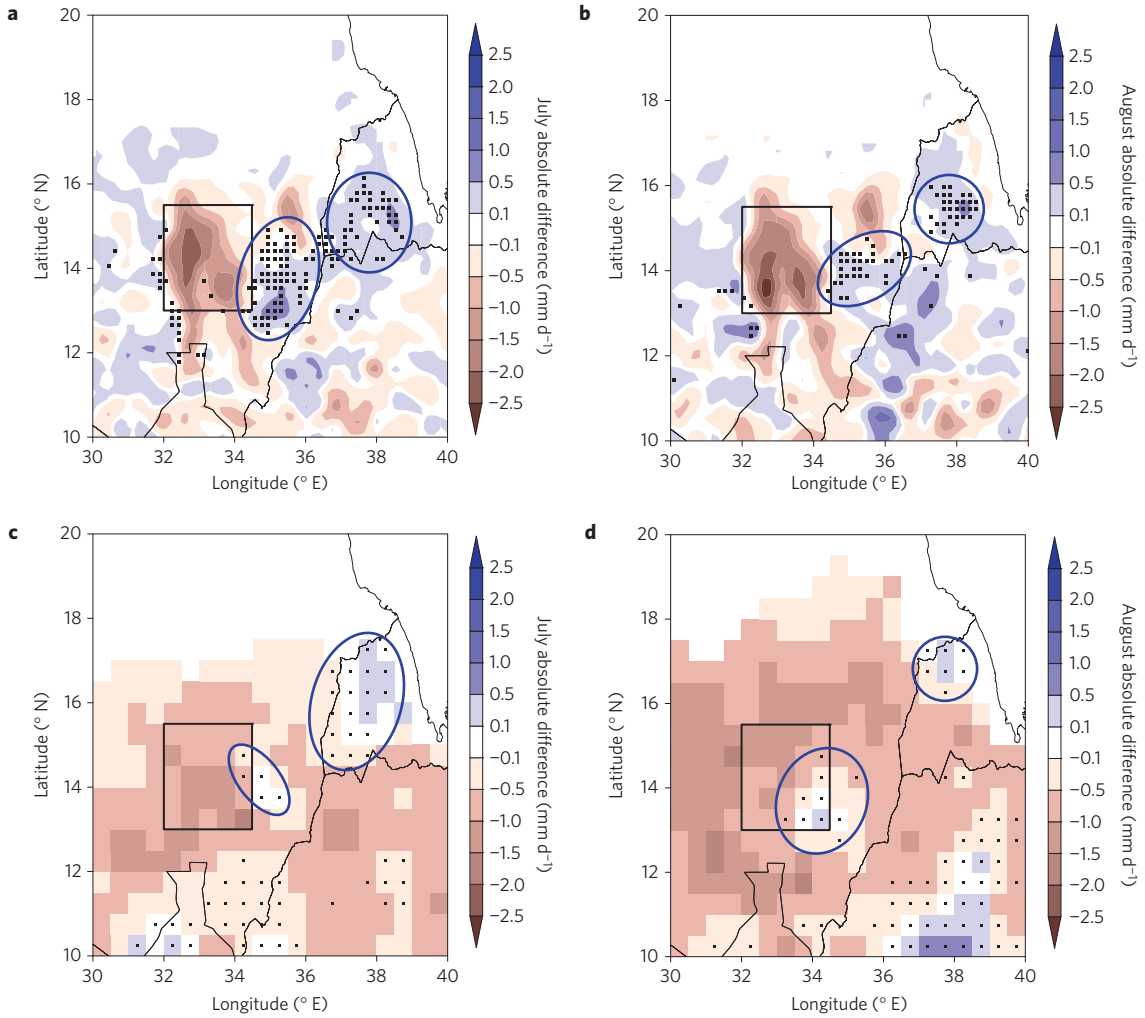

Figure 2 | Comparison of simulated and observed changes in rainfall. a,**b**, Absolute difference in ensemble mean rainfall between irrigation (IRR) and control (CONT) simulations for July (**a**) and August (**b**). Superimposed dots indicate irrigation-induced rainfall enhancement during at least 70% of the ensemble years. **c**,**d**, Absolute difference in observed rainfall from pre-MEX to post-MEX for July (**c**) and August (**d**). Superimposed dots indicate grid cells where the value of a rainfall change consistency index $\geq$ 80th percentile (see Methods). Areas with mean CONT or pre-MEX rainfall $< 1\,\mathrm{mm\,d^{-1}}$ are masked out to avoid potential inflation due to small rainfall amounts.

by relative increases in rainfall east of Gezira (Gedaref—non-irrigated), and one minimally affected by irrigation west of Gezira (Kordofan—non-irrigated). The temporal evolution of surface air temperature shows that irrigated Gezira became significantly cooler than non-irrigated Kordofan post-MEX during July–August, and rainfall-affected Gedaref became cooler than Gezira (Fig. 4—see Methods for details). These temporal changes reinforce the notion that irrigation expansion in Gezira led to a robust modification of the surface energy budget.

Spatial changes in wind patterns are also analysed to investigate how irrigation in Gezira may be linked to circulation changes in the lower troposphere. Spatial maps of simulated wind anomalies at 925 hPa caused by irrigation in Gezira depict a weak clockwise circulation around the irrigated area during July and August (Fig. 4a), indicative of anomalously high surface pressure and agreeing with the wind fields of previous studies of irrigation impacts in the West African Sahel[13,14].

Finally, we investigated the potential impact of irrigation-induced rainfall on regional streamflow. Streamflow records from 1965 to 1999 indicate that the Atbara River (a tributary of the Nile east of Gezira) exhibited a greater increase in normalized streamflow than any other major tributary of the Nile River (Supplementary Fig. 5). As irrigation seems to enhance rainfall up to several hundred kilometres east of Gezira, this streamflow trend may be indicative of irrigation-induced rainfall enhancement over the Atbara River basin.

The results obtained from the above analyses fit into the mechanistic framework developed by previous studies over West Africa[13,14] and other parts of the world[8,10,12,19] that links irrigation to rainfall enhancement (see Supplementary Fig. 6 and Supplementary Information). Irrigation decreases surface air temperature and stabilizes the lower troposphere, causing anomalous subsidence and greater surface pressure over the irrigated areas. The resulting clockwise wind anomalies would cause horizontal convergence with the southwesterly background wind (not shown) to the south and east of the irrigated area, increasing upward vertical motion and, therefore, rainfall. Furthermore, greater values of specific humidity in this area (Fig. 4a) create a more favourable environment for rainfall enhancement. Within this mechanistic framework, both the regional climate model simulations and observation-based analyses seem to arrive at the same conclusion: irrigation development in the Gezira Scheme has consistently enhanced rainfall to the east of the irrigated areas and reduced rainfall directly over the irrigated areas.

This causative link between irrigation development and rainfall modification may have numerous implications for agricultural,

© 2015 Macmillan Publishers Limited. All rights reserved

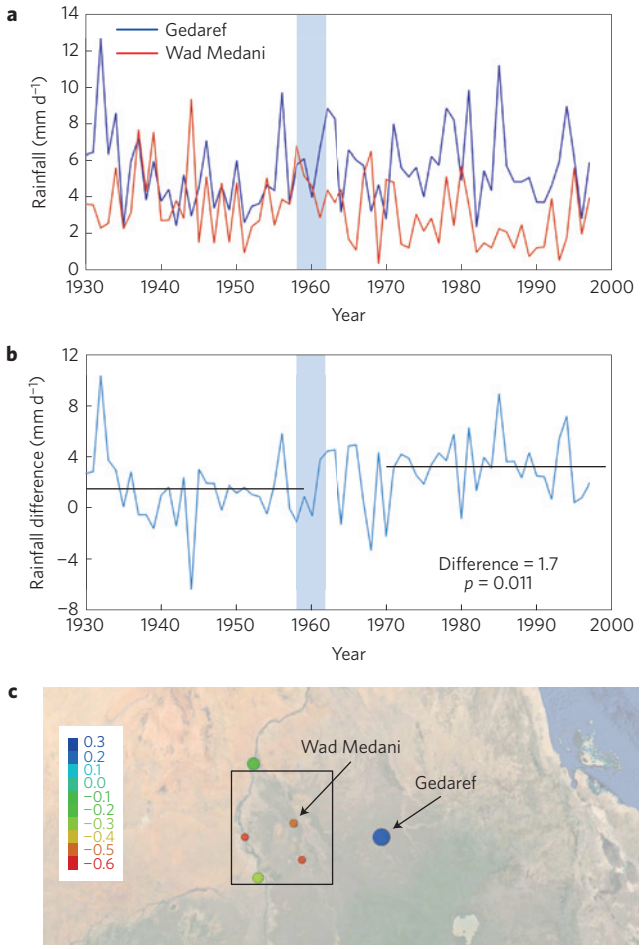

Figure 3 | Temporal and spatial changes in rainfall from station observations. a, Temporal evolution of observed July rainfall (mm d^{-1}) at Gedaref (non-irrigated) and Wad Medani (irrigated). The blue vertical bar represents the Manaqil Extension (MEX). **b**, Temporal evolution of the difference in July rainfall between Gedaref and Wad Medani. Black horizontal lines represent the mean inter-station difference for pre-MEX (1930–1959) and post-MEX (1970–1999). The absolute change between the horizontal lines and its *p*-value are located in the bottom right corner of the panel. **c**, Spatial distribution of the change in normalized rainfall (unitless) for six long-term stations from pre-MEX to post-MEX.

hydrologic, economic and political interests both inside and outside these irrigated areas. Enhanced rainfall due to irrigation in the Gezira Scheme could improve agricultural productivity, economic prosperity, and food and water availability in the regions to the south and east of Gezira (for example, Gedaref), which already support wide swaths of rain-fed agriculture (Supplementary Fig. 1). On the other hand, reduced rainfall over the irrigated areas probably necessitates additional water withdrawal for irrigation, forming a feedback loop that could ultimately reduce the hydrologic and economic sustainability of irrigation in the area. This wide spectrum of potential impacts warrants further consideration in plans to adapt to and mitigate regional effects of climate change.

Methods

Methods and any associated references are available in the online version of the paper.

Received 9 March 2015; accepted 20 July 2015; published online 7 September 2015

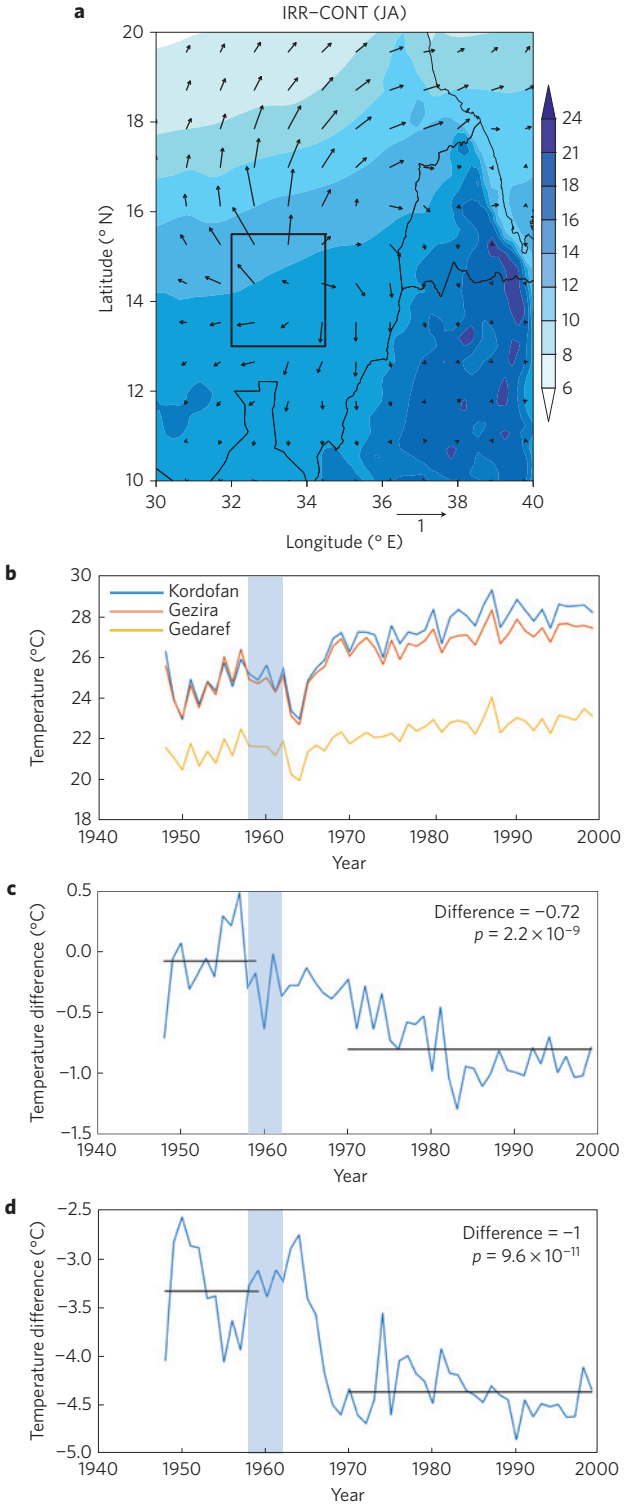

Figure 4 | Spatial changes in horizontal wind and temporal changes in surface air temperature. a, Simulated wind vector anomalies in m s^{-1} (IRR–CONT, arrows) and climatological values of specific humidity in g kg^{-1} (CONT, shaded) at the 925 hPa pressure level. **b**, Time series of July–August NCEP–NCAR reanalysis surface air temperature (°C) for grid cells over Kordofan (non-irrigated, west of Gezira), Gezira (irrigated) and Gedaref (non-irrigated, east of Gezira). **c**, Difference in July–August surface air temperature between Gezira and Kordofan. **d**, Difference in July–August surface air temperature between Gedaref and Gezira. In **c**,**d**, the absolute change between the horizontal lines and its *p*-value are located in the top right corner of the panel.

© 2015 Macmillan Publishers Limited. All rights reserved

References

1. Pielke, R. A. Sr *et al.* Land use/land cover changes and climate: Modeling analysis and observational evidence. *WIREs Clim. Change* **2,** 828–850 (2011).
2. Mahmood, R. *et al.* Land cover changes and their biogeophysical effects on climate. *Int. J. Climatol.* **34,** 929–953 (2014).
3. Stidd, C. K. Irrigation increases rainfall? *Science* **188,** 279–281 (1975).
4. Barnston, A. G. & Schickedanz, P. T. The effect of irrigation on warm season precipitation in the Southern Great Plains. *J. Clim. Appl. Meteorol.* **23,** 865–888 (1984).
5. Douglas, E. M., Beltrán-Przekurat, A., Niyogi, D., Pielke, R. A. Sr & Vörösmarty, C. J. The impact of agricultural intensification and irrigation on land–atmosphere interactions and Indian monsoon precipitation—A mesoscale modeling perspective. *Glob. Planet. Change* **67,** 117–128 (2009).
6. DeAngelis, A. *et al.* Evidence of enhanced precipitation due to irrigation over the Great Plains of the United States. *J. Geophys. Res.* **115,** D15115 (2010).
7. Puma, M. J. & Cook, B. I. Effects of irrigation on global climate during the 20th century. *J. Geophys. Res.* **115,** D16120 (2010).
8. Harding, K. J. & Snyder, P. K. Modeling the atmospheric response to irrigation in the Great Plains. Part I: General impacts on precipitation and the energy budget. *J. Hydrometeorol.* **13,** 1667–1686 (2012).
9. Qian, Y., Huang, M., Yang, B. & Berg, L. K. A modeling study of irrigation effects on surface fluxes and land–air–cloud interactions in the Southern Great Plains. *J. Hydrometeorol.* **14,** 700–721 (2013).
10. Lo, M. & Famiglietti, J. S. Irrigation in California's Central Valley strengthens the southwestern U. S. water cycle. *Geophys. Res. Lett.* **40,** 301–306 (2013).
11. Wei, J., Dirmeyer, P. A., Wisser, D., Bosilovich, M. G. & Mocko, D. M. Where does the irrigation water go? An estimate of the contribution of irrigation to precipitation using MERRA. *J. Hydrometeorol.* **14,** 275–289 (2013).
12. Huber, D., Mechem, D. & Brunsell, N. The effects of Great Plains irrigation on the surface energy balance, regional circulation, and precipitation. *Climate* **2,** 103–128 (2014).
13. Im, E.-S. & Eltahir, E. A. B. Enhancement of rainfall and runoff upstream from irrigation location in a climate model of West Africa. *Wat. Resour. Res.* **50,** 8651–8674 (2014).
14. Im, E.-S., Marcella, M. P. & Eltahir, E. A. B. Impact of potential large-scale irrigation on the West African monsoon and its dependence on location of irrigated area. *J. Clim.* **27,** 994–1009 (2014).
15. Xue, Y. Biosphere feedback on regional climate in tropical north Africa. *Q. J. R. Meteorol. Soc. B* **123,** 1483–1515 (1997).
16. Eltahir, E. A. B. A soil moisture-rainfall feedback mechanism: 1. Theory and observations. *Wat. Resour. Res.* **34,** 765–776 (1998).
17. Pielke, R. A. Sr Influence of the spatial distribution of vegetation and soils on the prediction of cumulus convective rainfall. *Rev. Geophys.* **39,** 151–177 (2001).
18. Kueppers, L. M., Snyder, M. A. & Sloan, L. C. Irrigation cooling effect: Regional climate forcing by land-use change. *Geophys. Res. Lett.* **34,** L03703 (2007).
19. Lee, E., Sacks, W. J., Chase, T. N. & Foley, J. A. Simulated impacts of irrigation on the atmospheric circulation over Asia. *J. Geophys. Res.* **116,** D08114 (2011).
20. Ozdogan, M., Rodell, M., Beaudoing, H. K. & Toll, D. L. Simulating the effects of irrigation over the United States in a land surface model based on satellite-derived agricultural data. *J. Hydrometeorol.* **11,** 171–184 (2010).
21. Mahmood, R., Hubbard, K. G., Leeper, R. D. & Foster, S. A. Increase in near-surface atmospheric moisture content due to land use changes: Evidence from the observed dewpoint temperature data. *Mon. Weath. Rev.* **136,** 1554–1561 (2008).
22. You, L. *et al. What is the Irrigation Potential for Africa? A Combined Biophysical and Socioeconomic Approach* Discussion Paper 00993 (International Food Policy Research Institute, 2010).
23. *World Development Indicators* (*WDI*) *Section 4: Economy* (The World Bank, 2010); http://data.worldbank.org/data-catalog/world-development-indicators/wdi-2010
24. Im, E.-S., Gianotti, R. L. & Eltahir, E. A. B. Improving simulation of the West African monsoon using the MIT Regional Climate Model. *J. Clim.* **27,** 2209–2229 (2014).
25. Plusquellec, H. *The Gezira Irrigation Scheme in Sudan: Objectives, Design, and Performance* (The World Bank, 1990); http://documents.worldbank.org/curated/en/1990/05/439697/gezira-irrigation-scheme-sudan-objectives-design-performance
26. NASA Land Processes Distributed Active Archive Center (LP DAAC) *MODIS Aqua MOD 11* (USGS/Earth Resources Observation and Science (EROS) Center, 2014).
27. Willmott, C. J. & Matsuura, K. *Terrestrial Precipitation: Gridded Monthly Time Series* (*1900–2010*) v.3.01 (Center for Climatic Research, Univ. Delaware, 15 October 2014); http://climate.geog.udel.edu/~climate/html_pages/Global2011/README.GlobalTsP2011.html
28. Peterson, T. C. & Vose, R. S. An overview of the Global Historical Climatology Network temperature database. *Bull. Am. Meteorol. Soc.* **78,** 2837–2849 (1997).
29. Kalnay, E. *et al.* The NCEP/NCAR 40-year reanalysis project. *Bull. Am. Meteorol. Soc.* **77,** 437–470 (1996).

Acknowledgements

Funding for this research was provided by the Cooperative Agreement between the Masdar Institute of Science and Technology (Masdar Institute) and the Massachusetts Institute of Technology (MIT), and by the Singapore–Massachusetts Institute of Technology Alliance for Research and Technology (SMART). We are grateful to M. Siam and the other members of the Eltahir Research Group for their support and valuable feedback.

Author contributions

E.A.B.E. conceived and supervised the study. E.-S.I. performed the numerical modelling experiments and analysis. R.E.A. performed the observational analyses. R.E.A. wrote the paper, with input from E.-S.I. and E.A.B.E. All authors discussed the results and commented on the manuscript.

Additional information

Supplementary information is available in the online version of the paper. Reprints and permissions information is available online at www.nature.com/reprints. Correspondence and requests for materials should be addressed to R.E.A. or E.-S.I.

Competing financial interests

The authors declare no competing financial interests.

© 2015 Macmillan Publishers Limited. All rights reserved

Methods

Regional climate model description. In this study, the MIT Regional Climate Model (MRCM) is used to examine the climatological effects of irrigation within the Gezira region of Sudan. MRCM maintains much of the structure of the Regional Climate Model version 3 (RegCM3; ref. 30), but with several improvements, including coupling to the IBIS land surface scheme[31], a new bare soil albedo assignment method[32], new convective cloud and convective rainfall autoconversion schemes[33,34], and modified boundary layer height and boundary layer cloud schemes[35]. In particular, a new irrigation module has been implemented within the IBIS land surface scheme[32], where root zone soil moisture is wetted to relative field capacity during each model time step. Similar approaches to modelling irrigation via saturation to field capacity have been widely implemented within various regional modelling studies[8,18,36–38]. Details on the workings of the irrigation module can be found in a previous study that implemented the module over West Africa[39].

Previous work has confirmed that MRCM can successfully simulate African climatic conditions during the summer[24], with significant improvement compared to other previous studies. Moreover, several sensitivity studies in West Africa have confirmed that using the irrigation scheme in simulations with MRCM produces physically feasible changes to regional energy and moisture budgets[13,14,39]. Given these validations, we adopted the same version of MRCM and designed the experiment to mimic the Gezira irrigation scheme in Sudan. A more detailed model description and the general performance of MRCM can be found in previous studies of MRCM simulations over West Africa[13,14,24,39].

Design of numerical experiments. The original model domain for the MRCM control simulation (CONT) covers most of Sudan, Ethiopia and Eritrea. It is centred at 13° N and 33.5° E with 20 km horizontal grid increments (152 grid points zonally and 104 grid points meridionally) and 18 vertical sigma levels from the surface to the 50 hPa level. The size of the domain and location of the boundaries were chosen to minimize interference from elevated topography to the south, yet also include the bulk of regional weather and climate patterns that affect East Africa. However, for presentation clarity, the figures in the paper are shown in a smaller model subdomain—namely, 10°–20° N and 30°–40° E.

Figure 1a presents the smaller model subdomain and land-use distribution for the sensitivity experiment that includes irrigation (IRR). The IRR simulation has an identical land-use configuration to the CONT simulation except for the 142 grid cells over the Gezira and New Halfa irrigation schemes that are designated as 'irrigated cropland'. The irrigated grid cell distribution was determined manually through Geographic Information System using visible satellite data. The threshold for classifying a grid cell as 'irrigated' was purposely liberal—25% or more irrigated coverage—to increase the detectability of signals in the simulated energy and moisture budgets. At grid cells that are designated as 'irrigated cropland', the irrigation module adds water to the root zone (top 1 m of the soil) at every time step until it reaches relative soil saturation, which is assumed to be relative field capacity, that is, field capacity divided by the porosity of a soil layer. Therefore, root zone soil moisture is maintained at relative field capacity throughout the irrigated time period.

The simulations span 30 years continuously from January 1979 to December 2008. The initial and boundary conditions used by MRCM are specified according to the ERA-Interim reanalysis[40]—the third generation ECMWF reanalysis project—which has horizontal grid increments of 1.5° × 1.5° at 6-h intervals. Although additional spin-up time is not added, this should not introduce a significant error because initial soil moisture conditions are specified from long-term offline simulations that bring soil moisture in equilibrium with the climate of the region. Sea surface temperature (SST) is prescribed by two data sets: the Met Office Hadley Centre's Global Sea Ice and Sea Surface Temperature (GISST; ref. 41) data set with monthly temporal resolution for the years 1979 to 1981, and the National Oceanic and Atmospheric Administration (NOAA) Optimum Interpolation (OI; ref. 42) SST data set with horizontal grid increments of 1° × 1° and weekly temporal resolution for the remaining time period (1982 to 2008). To minimize the dependence of the model simulations on initial conditions, we also performed two additional experiments with different starting dates (that is, additional starting times of 1979.1.2 and 1979.1.3) to generate time-lagged ensemble members. The climatological response to irrigation derived from the IRR simulations is based on the arithmetic mean of the three ensemble members.

Validation of the CONT simulation was performed with the University of Delaware gridded observational data set[27].

Statistical methodology and rationale. The main contribution of this paper is to present observational evidence documenting the impact of irrigation on climate in East Africa, at spatial scales of 10^3 to 10^5 km^2. However, any impact of irrigation at those scales would have taken place against the background of a severe drought in the late twentieth century[43,44], when strong decreases in rainfall covered the whole Sahel region at spatial scales of 10^6 km^2. This background drying trend complicates the detection of irrigation-induced impacts on regional climate in our study area.

As we expected that irrigation-induced increases in rainfall would be small compared to the above large-scale trends (indeed, we note that the mean simulated rainfall increase is only 5–20%), we focused less on the robustness of the magnitude of change and more on the robustness of the consistency of change. 'Traditional' two-sample, two-tailed Student t-tests identify only whether the magnitude of change shifts past a statistical threshold, so we instead chose to apply two different statistical tests that attempt to identify whether irrigation has consistently enhanced rainfall in the study region.

For the simulations, we decided to use the chi-square test (χ^2) to determine the consistency of the rainfall increases. The chi-square test analyses categorical data (for example, positive versus negative) to determine whether the distribution of categories is different enough from the expected outcome to reject the null hypothesis. In our case, the null hypothesis is that the distribution of positive and negative rainfall changes in the irrigation simulation is similar to the expectation of 50% positive and 50% negative changes. The dots in the simulation results (Fig. 2 and Supplementary Fig. 3) denote grid cells with irrigation-induced rainfall increases during at least 70% of the model years. The chi-square test calculates that $p = 0.006$ for this 70% consistency threshold. Therefore, in the grid cells that are covered by these dots, the consistency of the increases in irrigation-induced rainfall is statistically significant at the 1% level.

For the observations, we created a new statistic—the consistency of relative change index (CRCI)—that can be used to determine the consistency of the sign of relative change for any temporal variable. For this study, the CRCI is used to determine how frequently rainfall exhibits relative increases during a post-irrigation period compared to a pre-irrigation period. In general, the CRCI is calculated by counting the number of times that rainfall values in the later period (for example, post-MEX) exceed the mean of the observed rainfall in the earlier period (for example, pre-MEX). In this respect, the mean rainfall of the earlier period (for example, pre-MEX) is used as a threshold for determining how often the later period contains positive or negative rainfall anomalies. The CRCI can then be sorted by percentile rank for each grid cell value in relation to the corresponding values associated with all grid cells in the study area. In Fig. 2 and Supplementary Fig. 3, we identify with dots all grid cells where the CRCI is greater than or equal to the 80th percentile—that is, greater than 80% of all grid cell values.

Observational data. MODIS. Daytime land surface temperature data were obtained from the Moderate Resolution Infrared Spectrometer (MODIS) product MOD 11 on the Aqua satellite[26]. The data set is gridded to 0.05° × 0.05° horizontal grid increments.

UDel. The University of Delaware (UDel) precipitation data set version 3.01 (ref. 27) contains monthly totals of precipitation gridded to 0.5° × 0.5° horizontal grid increments from 1900 to 2010. The years 1930–1959 and 1970–1999 were chosen for rainfall comparison for several reasons: they both encompass 30 years, which is a generally acceptable length of time for deriving a 'climatology'; they both generally avoid the Manaqil Extension (MEX) time period (1958–1962), and the later time period allows a buffer of eight years post-MEX for any longer-period climatic signals to develop; a multi-decadal drought developed in the African Sahel beginning in the late 1960s[43,44], and the second time period avoids any potential overlap with this critical climatic shift; more frequent missing data during the early 1900s and 2000s within the GHCN data set prompted the data cutoffs to be 1930 and 1999 instead of 1900 and 2010, respectively (although there are missing data for July 1998 and August 1995); and beginning the data in 1930 avoids the marked increase in irrigation from its inception in 1925 until 1930.

It should be noted that the spatial patterns in UDel rainfall changes remain almost the same even when an earlier 1900–1929 time period is compared to the 1970–1999 time period. The main differences are smaller contrasts between the two clusters of relative rainfall increase and the background climate, and more relatively positive anomalies (although not of the same magnitude) in the eastern part of the domain (not shown). Analysing the temporal evolution of the rainfall difference between grid cells closest to Gedaref and Wad Medani from the 1900–1929 and 1970–1999 periods yields positive but not statistically significant changes during July and August.

In Fig. 2c,d and Supplementary Fig. 3c,d, the distinctly positive precipitation anomaly in the northeast corner of the domain is adjacent to two masked (whited-out) areas: the Red Sea to the northeast (which has no observations through UDel) and the regions of the domain to the northwest that typically receive less than 1 mm d^{-1} of rainfall. It should be noted that extending the domain eastward into the Arabian Peninsula and removing the <1 mm d^{-1} rainfall mask reveals positive rainfall anomalies in the Arabian Peninsula, but not of the magnitude shown in the northeast domain anomaly (not shown). The percentage changes in rainfall to the north of the positive rainfall anomaly are generally negative and further define the positive anomaly northeast of Gezira (not shown).

GHCN. Monthly precipitation data from the Global Historical Climatology Network (GHCN) version 2 (ref. 28) are station-based and were obtained through the National Climatic Data Center website. In this study, the GHCN data are also compared over the years 1930–1959 and 1970–1999, the same time periods as for the UDel data set.

© 2015 Macmillan Publishers Limited. All rights reserved

Although the UDel data set already assimilates available precipitation observations into a moderate-resolution spatial grid, we complemented this analysis with the GHCN data set as it is the only publicly available data set (to our knowledge) with long-term station observations of precipitation in Sudan.

All of the GHCN monthly precipitation data are run through various quality control tests before being made available to the public. However, the main caveat with GHCN data from Sudan stations is that they are not adjusted for systematic biases resulting from instrument and/or reporting changes that may have occurred over the period of record for a particular station. We still used the GHCN data set for this study as it provides the only available long-term, station data in Sudan, but we acknowledge that the results may be affected by inconsistencies in data homogeneity.

To minimize the potential influence of these inhomogeneities, we chose only long-term GHCN stations in the Gezira area with at least 50 years of data for our analyses. Both the Gedaref and Wad Medani stations, which are used in Fig. 3 and Supplementary Fig. 4, have more than 100 years of data. We compared the rainfall differences between these two stations with both the UDel and GHCN data sets (not shown), using the grid cells in UDel closest to Gedaref and Wad Medani. This analysis yields strong correlations between the UDel and GHCN time series, with $r = 0.85$ for both July and August. Thus, we feel confident that the potential loss of data quality due to using raw GHCN data does not significantly affect the robustness of our conclusions regarding observed rainfall changes.

NCEP–NCAR. In this study, we used monthly composites from the NCEP–NCAR Reanalysis[29], which is gridded to $2.5^\circ \times 2.5^\circ$ horizontal grid increments and begins in 1948. We analysed temperature data from this reanalysis over the years 1948–1959 and 1970–1999, which correspond to the years of the UDel and GHCN studies but account for the later start year of the reanalysis. The three grid cells discussed in this study are located within the Sudanese states of Northern Kordofan (12.5°–15° N, 30°–32.5° E), Gezira (irrigated—12.5°–15° N, 32.5°–35° E), and Gedaref (12.5°–15° N, 35°–37.5° E).

Streamflow. Streamflow data are gauge-based and were obtained from the Ministry of Water Resources and Electricity of Sudan for the period 1965–1999.

Data access. The MODIS Aqua MOD 11 data product was obtained through the online Data Pool at the NASA Land Processes Distributed Active Archive Center (LP DAAC), USGS/Earth Resources Observation and Science (EROS) Center, Sioux Falls, South Dakota (https://lpdaac.usgs.gov/data_access). GHCN data were obtained from NOAA's National Climatic Data Center (http://www.ncdc.noaa.gov). The UDel gridded observational data set, NCEP–NCAR reanalysis data, and OI sea surface temperature data were provided by the NOAA/OAR/ESRL PSD, Boulder, Colorado, USA (http://www.esrl.noaa.gov/psd). ERA-Interim reanalysis data were obtained from the European Centre for Medium-Range Weather Forecasts (ECMWF) (http://www.ecmwf.int/en/research/climate-reanalysis/era-interim). GISST sea surface temperature data were obtained from the Met Office Hadley Centre for Climate Change (http://www.metoffice.gov.uk/hadobs/gisst). Temporal irrigation data were provided by the Ministry of Water Resources and Electricity of Sudan. We welcome any and all additional data requests.

Code availability. All computer code used to conduct the analyses in this paper is available on request.

References

30. Pal, J. S. *et al.* The ICTP RegCM3 and RegCNET: Regional climate modeling for the developing world. *Bull. Am. Meteorol. Soc.* **88,** 1395–1409 (2007).
31. Winter, J. M., Pal, J. S. & Eltahir, E. A. B. Coupling of Integrated Biosphere Simulator to Regional Climate Model Version 3. *J. Clim.* **22,** 2743–2756 (2009).
32. Marcella, M. P. *Biosphere—Atmosphere Interactions Over Semi-arid Regions: Modeling the Role of Mineral Aerosols and Irrigation in the Regional Climate System* PhD dissertation, Massachusetts Institute of Technology (2012).
33. Gianotti, R. L. & Eltahir, E. A. B. Regional climate modeling over the Maritime Continent. Part I: New parameterization for convective cloud fraction. *J. Clim.* **27,** 1488–1503 (2014).
34. Gianotti, R. L. & Eltahir, E. A. B. Regional climate modeling over the Maritime Continent. Part II: New parameterization for autoconversion of convective rainfall. *J. Clim.* **27,** 1504–1523 (2014).
35. Gianotti, R. L. *Convective Cloud and Rainfall Processes over the Maritime Continent: Simulation and Analysis of the Diurnal Cycle* PhD dissertation, Massachusetts Institute of Technology (2012).
36. Sorooshian, S., Li, J., Hus, K. & Gao, X. How significant is the impact of irrigation on the local hydroclimate in California's Central Valley? Comparison of model results with ground and remote-sensing data. *J. Geophys. Res.* **116,** D06102 (2011).
37. Sorooshian, S., Li, J., Hus, K. & Gao, X. Influence of irrigation schemes used in regional climate models on evapotranspiration estimation: Results and comparative studies from California's Central Valley agricultural regions. *J. Geophys. Res.* **117,** D06107 (2012).
38. Harding, K. J. & Snyder, P. K. Modeling the atmospheric response to irrigation in the Great Plains. Part II: The precipitation of irrigated water and changes in precipitation recycling. *J. Hydrometeorol.* **13,** 1687–1703 (2012).
39. Marcella, M. & Eltahir, E. A. B. Introducing an irrigation scheme to a regional climate model: A case study over West Africa. *J. Clim.* **27,** 5708–5723 (2014).
40. Uppala, S., Dee, D., Kobayashi, S., Berrisford, P. & Simmons, A. Towards a climate data assimilation system: Status update of ERA Interim. *ECMWF Newslett.* **115,** 12–18 (2008).
41. Rayner, N. A., Horton, E. B., Parker, D. E., Folland, C. K. & Hackett, R. B. *Version 2.2 of the Global Sea Ice and Sea Surface Temperature Data Set, 1903–1994 Clim. Res. Tech. Note CRTN74* (Hadley Centre, 1996).
42. Reynolds, R., Rayner, N. A., Smith, T. M., Stokes, D. C. & Wang, W. An improved *in situ* and satellite SST analysis for climate. *J. Clim.* **15,** 1609–1625 (2002).
43. Hoerling, M. P., Hurrell, J. W., Eischeid, J. & Phillips, A. Detection and attribution of twentieth-century northern and southern African rainfall change. *J. Clim.* **19,** 3989–4008 (2006).
44. Nicholson, S. E., Dezfuli, A. K. & Klotter, D. A two-century rainfall dataset for the continent of Africa. *Bull. Am. Meteorol. Soc.* **93,** 1219–1231 (2012).

© 2015 Macmillan Publishers Limited. All rights reserved